HHS Public Access

Author manuscript

Methods Mol Biol. Author manuscript; available in PMC 2017 January 01.

Published in final edited form as:

Methods Mol Biol. 2016 ; 1427: 243–262. doi:10.1007/978-1-4939-3615-1_14.

Neuroanatomical Tracing Techniques in the Ear: History, State of the Art, and Future Developments

Bernd Fritzsch, **Jeremy S. Duncan**, **Jennifer Kersigo**, **Brian Gray**, and **Karen L. Elliott**

Abstract

The inner ear has long been at the cutting edge of tract tracing techniques that have shaped and reshaped our understanding of the ear's innervation patterns. This review provides a historical framework to understand the importance of these techniques for ear innervation and for development of tracing techniques in general; it is hoped that lessons learned will help to quickly adopt transformative novel techniques and their information and correct past beliefs based on technical limitations. The technical part of the review presents details of our protocol as developed over the last 30 years. We also include arguments as to why these recommendations work best to generate the desired outcome of distinct fiber and cell labeling, and generate reliable data for any investigation. We specifically focus on two tracing techniques, in part developed and/or championed for ear innervation analysis: the low molecular multicolor dextran amine tract tracing technique and the multicolor tract tracing technique with lipophilic dyes.

Keywords

Neuronal tracing; Lipophilic dyes; Dextran amines; Ear; Innervation; Efferents; Afferents

1 Introduction

The inner ear, and more broadly the dorsolateral placode-derived system of mechano- and electrosensory organs, has been at the cutting edge of novel tracing techniques ever since Retzius adopted the Golgi technique to show that hair cells are contacted by nerve fibers derived from ganglia positioned between the ear and the brain [1]. The emerging neuron theory of Cajal was supported by showing hair cells are discontinuous from each other and neurons using the Golgi technique [2]. This finding conflicted sharply with the reticular hypothesis of Golgi himself [3]. Retzius also championed another technique that allowed him to show the entire pattern of innervation of vertebrate ears in unprecedented detail using osmium tetroxide for myelinated nerve fiber staining [4]. This technique continues to be

[10]Dextran amines diffuse only in live tissue [21] with a speed that depends on their molecular weight, but are also actively transported in vesicles in live tissue [56]. Labeling with dextran amines, therefore, needs to be conducted prior to any fixation either in vivo or as ex vivo explants such as the ear. The latter is possible simply because decay of tissue can be slower than filling with dextran amines under favorable circumstances, but care must be taken to avoid artifacts. The diffusion time of different dextran amines are directly related to their molecular weight [21] and should be taken into consideration when labeling neuronal populations as nerves are only viable after severance for a few hours in ex vivo preparations. Dextran amines can be effectively used for ex vivo tracing [39, 45] or in live embryos [35, 57], but care needs to be taken to avoid technical artifacts such as partial or incomplete filling of neurons and processes. If properly controlled, such an artifact of differential filling can be used to highlight specific fiber types over others in the developing cochlea [44]. However, we strongly recommend to carefully compare such data with other tracing data using different techniques such as lipophilic dyes in fixed tissue [23], to verify data generated by ex vivo dextran amine tracing.

used to show the distribution of myelinated nerve fibers in the ear today [5]. Not only was the myelinated nerve fiber staining an excellent technique to show the innervation in whole-mounted ears, but this approach facilitated the identification of distinct sensory epithelia. Comparative analysis of innervation patterning led to identifying the basilar papilla as a precursor for the organ of Corti as well as the amphibian papilla being a unique and unifying feature across for amphibians [4, 6].

Despite all the information provided by these early techniques, the “early masters” also made some profound mistakes in their interpretation as a consequence of technical limitations. For example, Retzius did not know that myelin will lose lipids through alcohol preservation and thus cannot be stained by osmium. Using such alcohol-treated specimens, he failed to identify nerve fibers to a ninth inner ear sensory epithelium only found in gymnophionans [7]. This lack of understanding the technique’s limitations led to a heated debate at its time [8, 9]. It took modern approaches to rectify this mistake [6] and demonstrate that the neglected and amphibian papilla are innervated by the same nerve twig, but are two parts of a single epithelium that end up in two different parts of the ear during development: the saccular recess (amphibian papilla aka saccular papilla) and the utricular recess (the neglected papilla aka utricular papilla). Even more profound were misinterpretations by Cajal (the master of Golgi staining) and his student, Lorente de No. Cajal stained fibers of what is now known as the olivo-cochlear bundle crossing in the hindbrain but believed this to be primary afferents forming an acoustic commissure similar to retinal fibers that cross to the contralateral side [10]. Lorente de No identified a rich variety of “afferent fibers” going to inner and outer hair cells, which he categorized into a multitude of fiber types [11, 12] not knowing that some of his more peculiar fiber types were in fact olivo-cochlear efferents, later identified using novel staining techniques for degenerating nerve fibers [13, 14]. While we now know that only two types of afferents and two types of efferents enter the organ of Corti [15], reaching that conclusion required applications of several new tracer techniques, each providing both lasting as well as sometimes transient insights.

Degeneration techniques in frogs implicated Purkinje cells as the source of efferent fibers to the ear. The first modern tract tracing technique, horseradish peroxidase (HRP) revealed this not to be true. The original reports implicating Purkinje fibers projecting to the inner ear were incorrect due to a technical error using evidence of degeneration of terminals as an indicator of connections [16]. Many first-generation retrograde fluorescent tracers to reach laboratories were injected into the ear and led to the identification of variably sized populations of extremely diverse cell types that were claimed to be efferents [17]. Only the detailed fiber tracings possible with HRP showed that efferents were distributed bilaterally in the brainstem of many vertebrates, and that efferents to the vestibular and cochlear/auditory endorgans exhibit various degrees of segregation [18]. Additionally, HRP was used to show that efferents are derived facial motoneurons that segregate through selective migration away from facial branchial motoneurons [19, 20]. However, it took the invention of multicolor tract tracing with dextran amines [21, 22] and lipophilic dyes [21, 23] to demonstrate beyond a doubt the distribution of efferents in the hindbrain and their segregation through differential migration from the facial branchial motoneurons [24].

Most problematic was the early use of Golgi staining to sort out development of inner and outer hair cell innervation. These “insights” were derived in part by the technical inability to recognize the four different afferent and efferent fiber types in early embryos. For example, despite the visual clarity and stunning details of Poljak and Lorente de No’s drawings [12, 25], they were unable to categorize what they considered a multitude of afferent types with unknown quantitative ratios to the two types of hair cells. Obviously, growth of the fibers running along outer hair cells was the easiest to follow and both got the progressive expansion of this fiber type right. Other researchers utilized these insights in order to interpret their TEM data, which would have been impossible to interpret otherwise given the limited overview provided by this technique. In large part, based on the inability to distinguish between different fiber types, ideas were proposed that aimed to interpret the data in a hypothetical context of transient efferent and afferent connections [26, 27]. These transient fibers were reported by some to persist in the adult system [28], thereby generating lasting debates. Only modern tracing techniques, which allow complete filling of fibers from a specific source, could distinguish between afferents and efferents and clarified that afferents and efferents arrive at hair cells nearly simultaneously and that growth of afferents and efferents to outer hair cells is also tightly correlated in time [29]. Indeed, without filling fibers from their respective sources such a distinction would be impossible to make, as later markers making afferents and efferents distinct from one another are not present during the early sorting phase. More recent techniques using molecular approaches to label fibers have largely confirmed the earlier tract tracing data [30]. Moreover, the bilateral distribution of efferents was finally solved, when nerve fibers were found in mammals to project across the floor plate [31] and neurons were found to migrate across the floor plate in chicken [32].

The peripheral fiber-sorting problem of afferents and efferents found its match by the significant challenge to sort the projection pattern of afferents into the hindbrain. Using simple silver techniques or even Golgi staining did not allow detailing both the peripheral source of a given fiber (or fibers) and its central presentation. Different sources of afferents from vestibular and auditory endorgans, including the lateral line, were all believed to mingle in a large area called the acoustico-lateral (or octavo-lateral) area of the hindbrain [33]. In contrast to these claims, Golgi staining already showed that the afferents of the cochlea ended in a topological fashion in the cochlear nuclei, projecting information from different parts of the cochlea (different sound frequencies) to different parts of the cochlear nuclei [12]. However, it took modern HRP tracing to demonstrate that afferents from different parts of the lateral-line and inner ear each ended in distinct and non-overlapping areas and that the lateral line system of many aquatic vertebrates consists of both mechanosensory and electrosensory modalities, each projecting into their own target area of the hindbrain [34, 35]. Another finding related to modern tracing techniques was the discovery that hair cells with opposite polarity are in general each connected to unique afferents that project to distinct areas of the hindbrain [36–38].

The gain of insights using modern tracing techniques should not be mistaken as an indication that our current techniques are not also prone to artifacts such as false positives and false negatives. Given the past history of misinterpretations based on technical limitations, one can only guess what might happen with our current “insights” once new techniques come on line. As with past techniques, the limits of current techniques and thus

the interpretations of data based on the “truth” revealed by them need to be understood to avoid entering data into the literature that require corrections that could have been avoided with proper precautions. As we present the detailed protocols below for dextran amine and lipophilic dye tracings in the ear, we also present our rationale for doing things the way we propose, minimizing known problems with these techniques exemplified in current and past publications.

2 Materials

2.1 Laboratory Equipment

1. Stereomicroscope with light source (*see* Note 1).
2. Peristaltic pump with 24–30G needles for perfusion of mice starting at embryonic day (E) 12.5 (*see* Note 2).
3. Sylgard (Dow-Corning, Midland, MI) coated petri dishes (variable sizes depending on application) for dissections (*see* Note 3).
4. Fine forceps and Vannas scissors for the dissection (Geuder G-19775, Heidelberg, Germany) (*see* Note 4).
5. Sealable glass containers for tissue storage (variable sizes depending on size of tissue).
6. Compresstome (Precisionary Instruments, Greenville, NC) (*see* Note 5).

2.2 Chemicals for Dextran and Lipophilic Dye Tracing

1. NeuroVue dye (Molecular Targeting Technologies, West Chester, PA) (*see* Note 6).
2. 3000 Molecular weight Dextran amine dye (Life Technologies, Grand Island, NY).
3. Fixation solution consisting of 4 % PFA made in 1× PBS and 0.3 M sucrose to preserve extracellular space (*see* Note 7).

---

[1]We strongly recommend a stereoscope with epifluorescent capacity to take images of application sites for documentation purposes. It is also advantageous to use an epifluorescent dissection scope for checking the diffusion of the dyes. After diffusion we recommend using confocal microscopy for image acquisition.

[2]In our experience the tissue preparation using transcardial perfusion is so far superior to immersion fixation that we strongly recommend the former approach.

[3]There are multiple ways to work with tissue, but we find sylgard-covered Petri dishes the easiest way to manipulate embryos or to cut dye wavers without dulling sharp and/or pointed tools.

[4]There are many suppliers on the market, but we found that the Geuder forceps and scissors are most useful for our techniques.

[5]We obtained better sections of fresh tissue with the compresstome compared to traditional vibratome sections. We do not recommend embedding tissue in any organic solvent to allow infiltration with wax, as this will invariably lead to a reduction in clarity of labeling and individual fibers will only be visible in a halo of washed out lipophilic dye. However, fixable dextran amines can be processed by these means or even methacrylate embedding without much negative effects.

[6]Since the dyes are photosensitive, store them in a cool dark area in their original package to minimize exposure to light and air.

[7]It is paramount to keep in mind that there is no easy way to avoid shrinking of the extracellular space with concomitant expansion of neurons [49], leading to rupture of the surrounding lipid bilayers of neurons. We highly recommend adding sucrose (0.3 M) to the perfusion to avoid excessively shrinking the extracellular space at the expense of neuron expansion [50, 51]. Increasing the concentration of PFA up to 10 % works also to fully preserve membranes and avoid any diffusion of lipophilic dyes out of ruptured membranes, as typically obtained with simple perfusion and most notably with immersion. If immersion is necessary, a 1 min pretreatment with 0.3 M sucrose followed by fixation in 4 % PFA is paramount to reduce membrane disruptions due to neuronal swelling [51].

4. Glycerol for mounting media (*see* Note 8).
5. Glass slide and coverslips.
6. 0.5 M EDTA in water.
7. 70 % Ethanol in water.

3 Methods

3.1 Dye Labeling

Two major techniques for neuronal tracing in vivo and in fixed tissue are dextran amine tract tracing [21, 35, 39, 40] and lipophilic dye tracing [41 – 43]. We will first describe the procedure for in vivo or ex vivo tract tracing (dextran amines) followed by the procedure for lipophilic dye tracing in aldehyde fixed tissue (NeuroVue).

3.1.1 Dextran Amine Dye Application in Live Animals—All experiments with animals should be approved by the institute's IACUC according to the guidelines set forth by the NIH. Dextran amines were introduced in 1986 [39, 40] and are now available in colors tuned to all wavelengths compatible with confocal imaging and conjugated to various sized dextrans (*see* Notes 9_11).

1. Dissolve dextran amine crystals in a drop of water until you have a saturated solution. Allow the edges of the water drop to recrystallize.
2. Pre-load a tungsten needle with a small amount of dye by dragging it across the recrystallized edge. The amounts of dye on the tip can be varied by multiple sweeps through the partially crystallized fluid. We prefer to load the needle with a bolus of dye about two to four times the diameter of a tungsten needle.
3. Anesthetize animals with appropriate anesthesia. For mice isoflurane works well, and for amphibians we recommend 0.02 % Benzocaine.
4. Determine the area for dye application under a dissecting scope. Gently open up the tissue with vannas scissors to expose the neuronal population (brain applications) or nerve you want to label.

---

[8] We have used glycerol extensively in the past and have non-recommendable experiences with some of the more recent clearing agents. It is important to realize that lipophilic dyes will diffuse out of membranes as membrane lipids are dissolved in organic clearing agents leading to a blurred appearance of nerve fibers [52] instead of the detailed fiber imaging possible when avoiding organic solvents [53, 54]. A good overview of modern clearing agents was recently published [55] that appears to work better than most other recently proposed clearing agents, including preservation of membranes for electron microscopy. In our hands, it leads to rapid loss of lipophilic dyes.

[9] Injection of dextran amines has the risk of dye expansion away from the injection site and this needs to be checked to guess the effective uptake area of dextran amines [56]. If at all possible, we suggest using a topical application rather than injections, to increase non-vesicular Golgi-like filling of fibers and neurons predominantly through passive dye diffusion along the concentration gradient inside the cell both retrograde and anterograde. It has been suggested that this procedure resembles chromatography, likely because sugar residues abound on the outside of cells slowing down diffusion relative to the inside of neurons [21].

[11] Instead of fluorescent dyes, the use of biocytin as a tracer is also possible. However, while biocytin is certainly small enough to fill even the tiniest branch of a neuron, it has one disadvantage compared to fluorescent dextran amines: it requires visualization using the high affinity of streptavidin to biotin. Streptavidin, when conjugated to HRP, is a very large molecule that cannot easily be used for whole mount staining. Larger molecular weight dextran amines are not recommended as they tend to label only larger caliber fibers and cells, much like HRP [21]. Smaller molecules such as rhodamine can also be used but are difficult to fix and can pass through disrupted neuronal membranes, in particular in ex vivo preparations, leading to false positive labeling.

5. Make a cut/incision and use the tungsten needle to apply immediately the dye to the cut axons. Hold needle in place to let the dye dissolve for approximately 3–4 s and rinse the area with PBS multiple times to wash away all excess dye. Rapid application after nerve cutting and thorough washing are crucial steps that retain only dye diffused into severed fibers to anterogradely, retrogradely, or transganglionically filled neurons.

6. Maintain the animals under a low dose of anesthesia while the dye diffuses or maintain ex vivo preparations in tissue culture medium [44, 45]. 3000 molecular weight dextran amine dyes diffuse at a rate of 2 mm/h at room temperature but the quality of labeling falls off steeply over distance. We do not exceed 3 h (or approximately 6 mm) to reliably label nearly all cut nerve fibers [32] (*see* Note 12).

7. Fully anesthetize, then perfuse the animal transcardially with fixation solution. Use immersion for small animals, such as *Xenopus* larvae or ex vivo preparations (*see* Note 13).

8. Prepare tissue as whole mounts [46] or sections using various embedding techniques, including methacrylate embedding [47].

3.1.2 NeuroVue Application in Fixed Tissue—NeuroVue dyes come in various colors suitable for all confocal laser wavelengths and allow, if combined with two photon microscopy, the segregation of up to six different colors for distinct labeling (Figs. 1, 2, 3, 4, 5, and 6) [41].

1. Animals/tissue should be transcardially perfused with fixation solution and allowed to incubate in fixation solution at 4 °C for a minimum of 24 h (*see* Note 13).

2. Determine a dye application site to selectively label the neuronal population under consideration using a dissecting scope (*see* Note 14).

---

12 Viability of the tissue for proper diffusion with or without transport is crucial. Do not attempt to label long distances in ex vivo fibers. Even labeling of a subpopulation is suspect of being incomplete in analogy with the Golgi technique that labeled only 1 % of neurons. As with Golgi staining, those fibers labeled tend to be completely labeled thus generating no indication of a labeling problem. Since ex vivo preparations can have a differential effect on viability and filling of different fiber types, compare the data to those derived from other techniques to verify the conclusions.

13 For transcardial perfusion, a syringe can be used; however, utilizing a small peristaltic pump with appropriately sized needles is preferred, to maintain a constant pressure as recommended [51]. For best results in all portions of this protocol, the perfusion fixation step should be performed. For example, we perfuse mice starting with E12.5 and older. The tissue can be stored in 4 % PFA at 4 °C for 1 day to 6 months as long as exposure to bright light is avoided. Dextran amines remain stable after fixation, but can be bleached and are difficult to use in thick brain tissue or whole mount (due to lower fluorescence intensity), in particular when using 488 nm excitable dyes that are within the range of tissue autofluorescence. We do not recommend combining them with gluteraldeyde fixation, as this increases the fluorescence of the tissue dramatically, essentially wiping out the contrast.

14 Like other lipid tracers such as DiI and related substances, Neurovue fills entire neurons from an application site through its membranes (Fig. 6) by passive diffusion within the lipid bilayer surrounding each intact neuron. It is therefore paramount that the neuronal anatomy is fully understood in terms of background of connections, in order to place the dye on the most appropriate nerve for a given analysis [41]. Placing a dye too close to the desired imaging location results in both lateral diffusion of the dye, causing labeling of unwanted cell types and uneven fluorescence along the neuronal tract. Extract all extraneous tissue for good visualization of the chosen site for dye placement. However, some surrounding tissue may need to be kept to stabilize the inserted dye, and to make sure the dye does not become physically dislodged. If labeling two separate neuronal populations with different dyes, the placement of the dyes can be sequentially staggered if diffusion differences vary. It is important to realize that axonal and dendritic filopodia can extend for 100 μm or more with limited content of small actin bundles that are difficult to image in whole-mounted tissue [58]. Using lipophilic dyes easily allows imaging of structures such as filopodia, even in whole-mounted cochlea (Figs. 1, 2, and 3), or studying the transformation of growth cones into synapses in whole-mounted or sectioned cochlear nuclei (Figs. 4 and 5).

3. Apply dye as far from the area of interest as possible (1–2 mm). Choose a site where other neuronal populations will not project to as the neuronal population under consideration. A good understanding of neuroanatomy helps in this process (*see* Note 14).

4. Cut the pre-loaded NeuroVue dye filter strips into appropriately sized triangular pieces with vannas scissors. The optimal size will be as small of a piece as possible, to avoid labeling other structures, while remaining large enough to label the population of interest and not become dislodged. The scissors used to cut the dye need to be rinsed in alcohol to remove dye residue and need to be clean of alcohol when cutting (70 % EtOH in water). This eliminates unintended contamination of tissue/cells with dye (*see* Note 15).

5. When inserting into soft tissue, such as the brain, we recommend to directly insert the filter using a point of the filter cut in a triangle to pierce the tissue (Fig. 1). This ensures the dye contacts all intended structures. For more rigid tissues, we suggest making an incision with scissors. Do not use a dissecting needle or other apparatus to push filter into tissues as this inadvertently leads to unintended labeling. For very small applications, we recommend compressing the filter wedge with forceps, to make the tip even sharper and the application site smaller.

6. Place the specimens in a securely closed vial with 4 % PFA and incubate at ~36–65 °C in the dark for 2–7 days, depending on age and diffusion distance to be covered (~2 mm per day at 65 °C). Elevated temperatures accelerate diffusion but also risk unusual labeling as membranes become unstable. We recommend parafilm to seal the container.

7. Verify that the dye has diffused to the desired location, and dissect out tissue of interest, using a dissecting scope with epifluorescence (*see* Note 16).

8. Whole mount the specimen on a slide with glycerol and coverslip for imaging with a confocal microscope (*see* Note 17). If tissue is too large to be mounted on a slide, either remove extraneous tissue or section tissue.

---

[15] It may be beneficial to use forceps to compress the dye filter strips, if they are too thick for the application, as this enhances the rigidity of the filter for easy piercing of the tissue. We do not recommend the use of crystals for these applications, as even the smallest amount of crystal can easily lead to unintended labeling of fiber, thus ruining the preparation. In particular, when using mutant mouse tissue, we do not recommend using crystals because of possible artifacts that could lead to misinterpretation, such as alleged mis-wiring that may be related to inadvertent labeling with small crystals. It is absolutely essential, in our hands, to take images of the application site at the time of application as well as after completion of the diffusion, to make sure that the intended application is indeed what was labeled (Fig. 1). Excellent data for controlling application problems are provided in several publications [54, 59]. Failing to provide images of application sites should result in rejection of papers by reviewers, in particular if aberrant wiring in the ear is claimed without being demonstrated, as we did in several of our papers [53, 59].

[16] Visualizing dye diffusion with epifluorescence will underestimate the diffusion of the dye seen with a confocal microscope, which is much more sensitive. Usually visualization of 50–75 % of the desired diffusion length will indicate the dye diffused to the area of interest to be imaged by confocal microscopy. If dye is allowed to diffuse until it can be visualized with epifluorescence at the area of interest, there will be quenching when using confocal imaging.

[17] Confocal settings can be gleaned from the information supplied with the dye or as described previously [41].

9. We found that sectioning with the compresstome leads to better results compared to vibratomes. However, both are suitable techniques to obtain thick (100–200 μm) sections.

10. Mount sections with spacers to avoid compression in 100 % glycerol. Our experience with other mounting media has been negative, except for Moviol.

11. Stay alert about future developments in tract tracing techniques using modern molecular approaches (*see* Note 18).

3.2 3-Dimensional Reconstruction

Tissues labeled with either dextran amine or lipophilic dyes or by immunohistochemistry can be subjected to 3-dimensional (3D) reconstruction of the confocal images obtained as described in [46, 48].

1. Perform dye tracing following protocols outlined above.

2. Decalcify tissue in ethylenediaminetetraacedic acid (EDTA) if bone is present.

3. Mount tissue in a clearing solution or glycerol. Use spacers or vacuum grease so that the tissue is not compressed and obtain confocal images.

4. Load the confocal file into Amira, Imaris, or similar 3D reconstruction software programs and manually segment the area(s) of interest to create a 3D rendering of the dye or immunohistochemistry stain.

Acknowledgments

Confocal images were obtained at the University of Iowa Carver Center for Imaging. We thank the Office of the Vice President for Research (OVPR), University of Iowa College of Liberal Arts and Sciences (CLAS), and the P30 core grant for support (DC 010362). This work was in part supported by a NASA base grant (Bernd Fritzsch) and 1R43GM108470-01 (Gray, Fritzsch).

References

1. Retzius G. Uber die peripherische Endigungsweise des Gehornerven. Biologische Untersuchungen. 1881; 3:1–51.
2. Ramón y Cajal S. Nobel lectures, physiology or medicine. 1906:1901–1921.
3. Golgi C. The neuron doctrine: theory and facts. Nobel Lecture. 1906; 1921:190–217.
4. Retzius G. Das Gehörorgan der Fische und Amphibien. Samson & Wallin, Stockholm. 1881
5. Kersigo J, Fritzsch B. Inner ear hair cells deteriorate in mice engineered to have no or diminished innervation. Front Aging Neurosci. 2015; 7:33. [PubMed: 25852547]

[18]Future directions—Tract tracing will always be used as a simple way to analyze mutant phenotypes or normal development without the need to do additional breeding, as is required with other techniques such as BRAINBOW [60] or CONFETI [61]. However, several new techniques are in the making that can potentially help to detail some of the open issues related to the development of fiber connections with hair cells. Cre-induced expression of various protein markers is a technique [30] that has recently been replaced by a next generation of fluorescent proteins that allow multicolor labeling [62], as demonstrated here with dextran amines and lipophilic dyes (Figs. 1 and 6). These approaches can be combined with high-resolution EM imaging, to obtain complete information about connections at the synaptic level [63], using correlated light and electron microscopy [64].

6. Fritzsch B, Wake M. The inner ear of gymnophione amphibians and its nerve supply: a comparative study of regressive events in a complex sensory system (Amphibia, Gymnophiona). Zoomorphol. 1988; 108(4):201–217.
7. Sarasin P, Sarasin F. Zur Entwicklungsgeschichte und Anatomie der ceylonesischen Blindwühle Ichthyophis glutinosus. Das Gehörorgan. Ergebnisse Naturwiss Forsch auf Ceylon, Bd 2. *Kreidels Verlag*. Wiesbaden. 1888
8. Sarasin P, Sarasin F. Über das Gehörorgan der Caeciliiden. Anat Anz. 1892; 7:812–815.
9. Retzius G. Das Gehörorgan von caecilia annulata. Anat Anz. 1891; 6:82–86.
10. Ramón y Cajal, S. Histology of the nervous system of man and vertebrates. Vol. 1. Oxford University Press; New York, USA: 1995.
11. Lorent De No, R. The primary acoustic nuclei. Raven Press; New York: 1981.
12. Lorente de No R. The sensory endings in the cochlea. Laryngoscope. 1937; 47:373–377.
13. Rasmussen GL. The olivary peduncle and other fiber projections of the superior olivary complex. J Comp Neurol. 1946; 84(2):141–219. [PubMed: 20982804]
14. Rasmussen GL. Further observations of the efferent cochlear bundle. J Comp Neurol. 1953; 99(1): 61–74. [PubMed: 13084783]
15. Brown M, Pierce S, Berglund A. Cochlear-nucleus branches of thick (medial) olivocochlear fibers in the mouse: a cochaleotopic projection. J Comp Neurol. 1991; 303(2):300–315. [PubMed: 2013642]
16. Hillman DE. Light and electron microscopical study of the relationships between the cerebellum and the vestibular organ of the frog. Exp Brain Res. 1969; 9(1):1–15. [PubMed: 5808479]
17. Strutz J, Schmidt CL, Stürmer C. Origin of efferent fibers of the vestibular apparatus in goldfish. A horseradish peroxidase study. Neurosci Letts. 1980; 18(1):5–9. [PubMed: 6189014]
18. Roberts BL, Meredith GE. The efferent innervation of the ear: variations on an enigma. In: DB Webster, RR Fay, AN Popper. The evolutionary biology of hearing. Springer, New York. 1992:185–121.
19. Fritzsch B, Wahnschaffe U. Electron microscopical evidence for common inner ear and lateral line efferents in urodeles. Neurosci Letts. 1987; 81(1):48–52. [PubMed: 2447525]
20. Sienknecht UJ, Köppl C, Fritzsch B. Evolution and development of hair cell polarity and efferent function in the inner ear. Brain Beh Evol. 2014; 83(2):150–161.
21. Fritzsch B. Fast axonal diffusion of 3000 molecular weight dextran amines. J Neurosci Meth. 1993; 50(1):95–103.
22. Hellmann B, Fritzsch B. Neuroa natomical and histochemical evidence for the presence of common lateral line and inner ear efferents and of efferents to the basilar papilla in a frog, *Xenopus laevis*. Brain Beh Evol. 1996; 47(4):185–194.
23. Simmons, D.; Duncan, J.; de Caprona, DC.; Fritzsch, B. Development of the inner ear efferent system. In: Ryugo, DK.; Fay, RR.; Popper, AN., editors. Auditory and vestibular efferents. Springer; New York: 2011. p. 187-216.
24. Yang T, Bassuk AG, Stricker S, Fritzsch B. Prickle1 is necessary for the caudal migration of murine facial branchiomotor neurons. Cell Tissue Res. 2014; 357(3):549–561. [PubMed: 24927917]
25. Poljak S. Über den allgemeinen Bauplan des Gehörsystems und über seine Bedeutung für die Physiologie, für die Klinik und für die Psychologie. Zeitschrift für die gesamte Neurologie und Psychiatrie. 1927; 110(1):1–49.
26. Echteler SM. Developmental segregation in the afferent projections to mammalian auditory hair cells. Proc Natl Acad Sci U S A. 1992; 89(14):6324–6327. [PubMed: 1631126]
27. Bulankina A, Moser T. Neural circuit development in the mammalian cochlea. Physiology. 2012; 27(2):100–112. [PubMed: 22505666]
28. Sobkowicz HM, August BK, Slapnick SM. Synaptic arrangements between inner hair cells and tunnel fibers in the mouse cochlea. Synapse. 2004; 52(4):299–315. [PubMed: 15103696]
29. Fritzsch B, Dillard M, Lavado A, Harvey NL, Jahan I. Canal cristae growth and fiber extension to the outer hair cells of the mouse ear require Proxl activity. PLoS One. 2010; 5:e9377. [PubMed: 20186345]

30. Koundakjian EJ, Appler JL, Goodrich LV. Auditory neurons make stereotyped wiring decisions before maturation of their targets. J Neurosci. 2007; 27(51):14078–14088. [PubMed: 18094247]
31. Cowan CA, Yokoyama N, Bianchi LM, Henkemeyer M, Fritzsch B. EphB2 guides axons at the midline and is necessary for normal vestibular function. Neuron. 2000; 26(2):417–430. [PubMed: 10839360]
32. Fritzsch B, Christensen M, Nichols D. Fiber pathways and positional changes in efferent perikarya of 2.5- to 7-day chick embryos as revealed with dil and dextran amiens. J Neurobiol. 1993; 24(11): 1481–1499. [PubMed: 7506749]
33. Ayers H, Worthington J. The finer anatomy of the brain of Bdellostoma dombeyi. I. The acustico-lateral system. Am J Anat. 1908; 8(1):1–16.
34. Fritzsch B. The pattern of lateral-line afferents in urodeles. Cell Tissue Res. 1981; 218(3):581–594. [PubMed: 7261043]
35. Fritzsch B, Gregory D, Rosa-Molinar E. The development of the hindbrain afferent projections in the axolotl: evidence for timing as a specific mechanism of afferent fiber sorting. Zoology. 2005; 108(4):297–306. [PubMed: 16351978]
36. Fritzsch B. Electroreceptors and direction specific arrangement in the lateral line system of salamanders? Zeitschrift für Naturforschung C. 1981; 36(5–6):493–496.
37. Maklad A, Kamel S, Wong E, Fritzsch B. Development and organization of polarity-specific segregation of primary vestibular afferent fibers in mice. Cell Tissue Res. 2010; 340(2):303–321. [PubMed: 20424840]
38. Fritzsch, B.; López-Schier, H. Evolution of polarized hair cells in aquatic vertebrates and their connection to directionally sensitive neurons. In: Bleckmann, H.; Mogdans, J.; Coombs, SL., editors. Flow sensing in air and water. Springer; New York: 2014. p. 271-294.
39. Glover J. Retrograde and anterograde axonal tracing with fluorescent dextran-amines in the embryonic nervous system. Neurosci Prot. 1995; 30:1–13.
40. Fritzsch B, Wilm C. Dextran amines in neuronal tracing. Trends Neurosci. 1990; 13(1):14. [PubMed: 1688669]
41. Tonniges J, Hansen M, Duncan J, Bassett MJ, Fritzsch B, Gray BD, Easwaran A, Nichols MG. Photo- and bio-physical characterization of novel violet and near-infrared lipophilic fluorophores for neuronal tracing. J Microsc. 2010; 239(2):117–134. [PubMed: 20629917]
42. Godement P, Vanselow J, Thanos S, Bonhoeffer F. A study in developing visual systems with a new method of staining neurones and their processes in fixed tissue. Development. 1987; 101(4): 697–713. [PubMed: 2460302]
43. Wilm C, Fritzsch B. Ipsilateral retinal projections into the tectum during regeneration of the optic nerve in the cichlid fish Haplochromis burtoni: a dil study in fixed tissue. J Neurobiol. 1992; 23(6): 692–707. [PubMed: 1431840]
44. Huang L-C, Thorne PR, Housley GD, Montgomery JM. Spatiotemporal definition of neurite outgrowth, refinement and retraction in the developing mouse cochlea. Development. 2007; 134(16):2925–2933. [PubMed: 17626062]
45. Bleckmann H, Niemann U, Fritzsch B. Peripheral and central aspects of the acoustic and lateral line system of a bottom dwelling catfish, Ancistrus sp. J Comp Neurol. 1991; 314(3):452–466. [PubMed: 1726106]
46. Elliott KL, Houston DW, DeCook R, Fritzsch B. Ear manipulations reveal a critical period for survival and dendritic development at the single- cell level in Mauthner neurons. Dev Neurobiol. 2015; doi: 10.1002/dneu.22287
47. Fritzsch B, Northcutt R. A plastic embedding technique for analyzing fluorescent dextran- amine labelled neuronal profiles. Biotech Histochem. 1992; 67(3):153–157. [PubMed: 1377506]
48. Kopecky BJ, Duncan JS, Elliott KL, Fritzsch B. Three-dimensional reconstructions from optical sections of thick mouse inner ears using confocal microscopy. J Microsc. 2012; 248(3):292–298. [PubMed: 23140378]
49. Thorne RG, Nicholson C. In vivo diffusion analysis with quantum dots and dextrans predicts the width of brain extracellular space. Proc Natl Acad Sci U S A. 2006; 103(14):5567–5572. [PubMed: 16567637]

50. Fritzsch B. Observations on degenerative changes of Purkinje cells during early development in mice and in normal and otocyst-deprived chickens. Anat Embryol. 1979; 158(1):95–102. [PubMed: 525827]
51. Cragg B. Preservation of extracellular space during fixation of the brain for electron microscopy. Tissue Cell. 1980; 12(1):63–72. [PubMed: 6987773]
52. Lu CC, Cao X-J, Wright S, Ma L, Oertel D, Goodrich LV. Mutation of Npr2 leads to blurred tonotopic organization of central auditory circuits in mice. PLoS Genetics. 2014; 10(12):e1004823. [PubMed: 25473838]
53. Jahan I, Kersigo J, Pan N, Fritzsch B. Neurod1 regulates survival and formation of connections in mouse ear and brain. Cell Tissue Res. 2010; 341(1):95–110. [PubMed: 20512592]
54. Maklad A, Fritzsch B. Partial segregation of posterior crista and saccular fibers to the nodulus and uvula of the cerebellum in mice, and its development. Dev Brain Res. 2003; 140(2):223–236. [PubMed: 12586428]
55. Costantini I, Ghobril J-P, Di Giovanna AP, et al. A versatile clearing agent for multi-modal brain imaging. Sci Rep. 2015; 5:9808. [PubMed: 25950610]
56. Tsuriel S, Gudes S, Draft RW, Binshtok AM, Lichtman JW. Multispectral labeling technique to map many neighboring axonal projections in the same tissue. Nat Methods. 2015; 12(6):547–552. [PubMed: 25915122]
57. Manns M, Fritzsch B. The eye in the brain: retinoic acid effects morphogenesis of the eye and pathway selection of axons but not the differentiation of the retina in *Xenopus* laevis. Neurosci Letts. 1991; 127(2):150–154. [PubMed: 1881624]
58. Gehler S, Gallo G, Veien E, Letourneau PC. p75 neurotrophin receptor signaling regulates growth cone filopodial dynamics through modulating RhoA activity. J Neurosci. 2004; 24(18):4363–4372. [PubMed: 15128850]
59. Pauley S, Lai E, Fritzsch B. Foxg1 is required for morphogenesis and histogenesis of the mammalian inner ear. Dev Dyn. 2006; 235(9):2470–2482. [PubMed: 16691564]
60. Cai D, Cohen KB, Luo T, Lichtman JW, Sanes JR. Improved tools for the Brainbow toolbox. Nat Methods. 2013; 10(6):540–547.
61. Abe T, Fujimori T. Reporter mouse lines for fluorescence imaging. Dev Growth Differ. 2013; 55(4):390–405. [PubMed: 23621623]
62. Viswanathan S, Williams ME, Bloss EB, et al. High-performance probes for light and electron microscopy. Nat Methods. 2015; 12:568–576. [PubMed: 25915120]
63. Mikula S, Denk W. High-resolution whole- brain staining for electron microscopic circuit reconstruction. Nat Methods. 2015; 12:541–546. [PubMed: 25867849]
64. de Boer P, Hoogenboom JP, Giepmans BN. Correlated light and electron microscopy: ultrastructure lights up! Nat Methods. 2015; 12(6):503–513. [PubMed: 26020503]
65. Fritzsch B. Development of inner ear afferent connections: forming primary neurons and connecting them to the developing sensory epithelia. Brain Res Bull. 2003; 60(5):423–433. [PubMed: 12787865]
66. Fritzsch B, Pan N, Jahan I, Elliott KL. Inner ear development: building a spiral ganglion and an organ of Corti out of unspecified ectoderm. Cell Tissue Res. 2015; 361:7–24. [PubMed: 25381571]
67. Maricich SM, Xia A, Mathes EL, Wang VY, Oghalai JS, Fritzsch B, Zoghbi HY. Atoh1- lineal neurons are required for hearing and for the survival of neurons in the spiral ganglion and brainstem accessory auditory nuclei. J Neurosci. 2009; 29(36):11123–11133. [PubMed: 19741118]

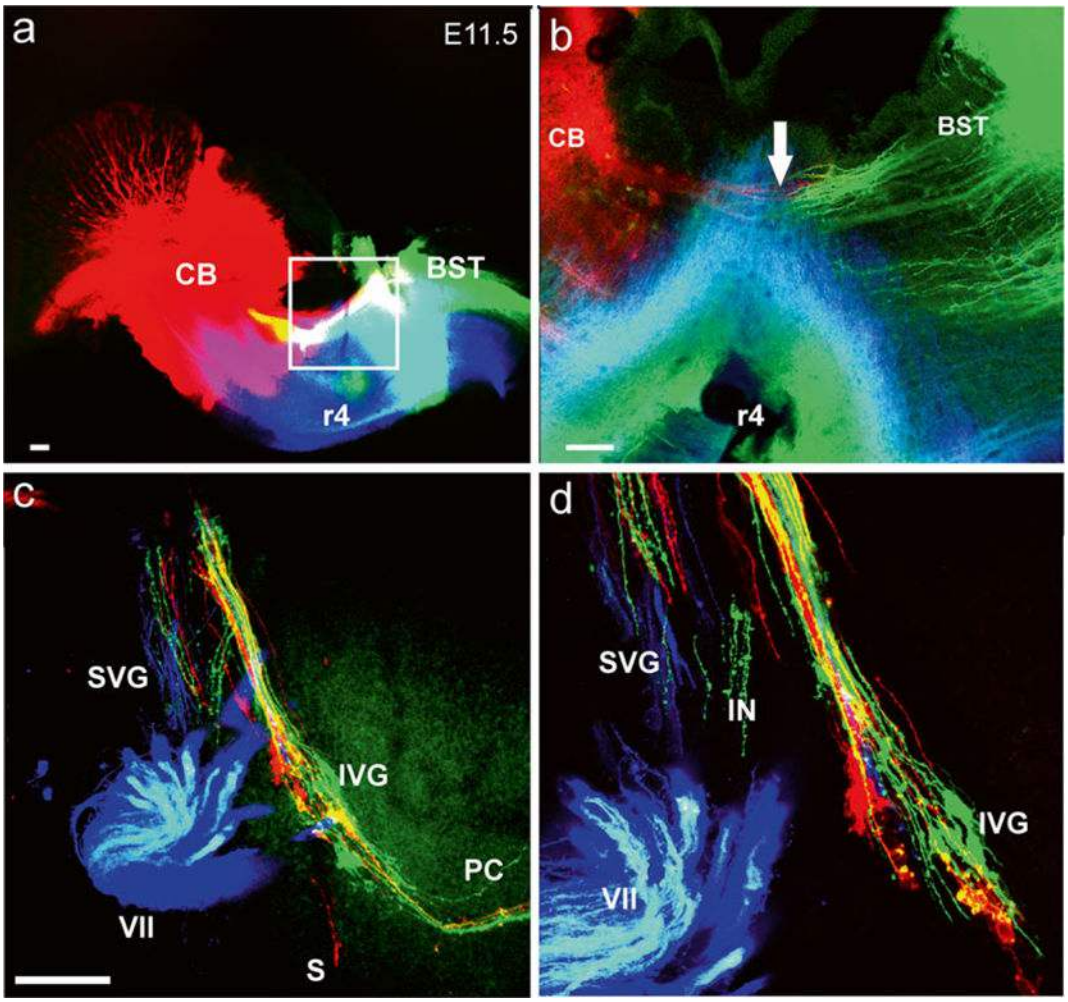

Fig. 1.

Early growth of afferents and efferents to the ear. Top images (**a**, **b**) show the injection sites of three different lipophilic dyes into the hemisected brainstem of an 11.5-day-old mouse embryo. *Green* is NeuroVue Jade, *red* is NeuroVue Orange, *blue* is NeuroVue Maroon. *Square* in (**a**) indicates position of (**b**). Note how brainstem (BST) and cerebellar (CB) afferents enter the VIII nerve (*arrow* in **b**). The whole-mounted ear (**c**, **d**) shows afferents filled from the cerebellum and brainstem (*red* and *green*) as well as efferents (*blue* to extend toward the targets). The higher power image shows the segregation different vestibular ganglion neurons. *IVG* inferior vestibular ganglion, *PC* posterior canal crista, *S* saccule, *SVG* superior vestibular ganglion, *VII* facial nerve, *r4* rhombomere 4. Bar indicates 100 μm. Modified after [38]

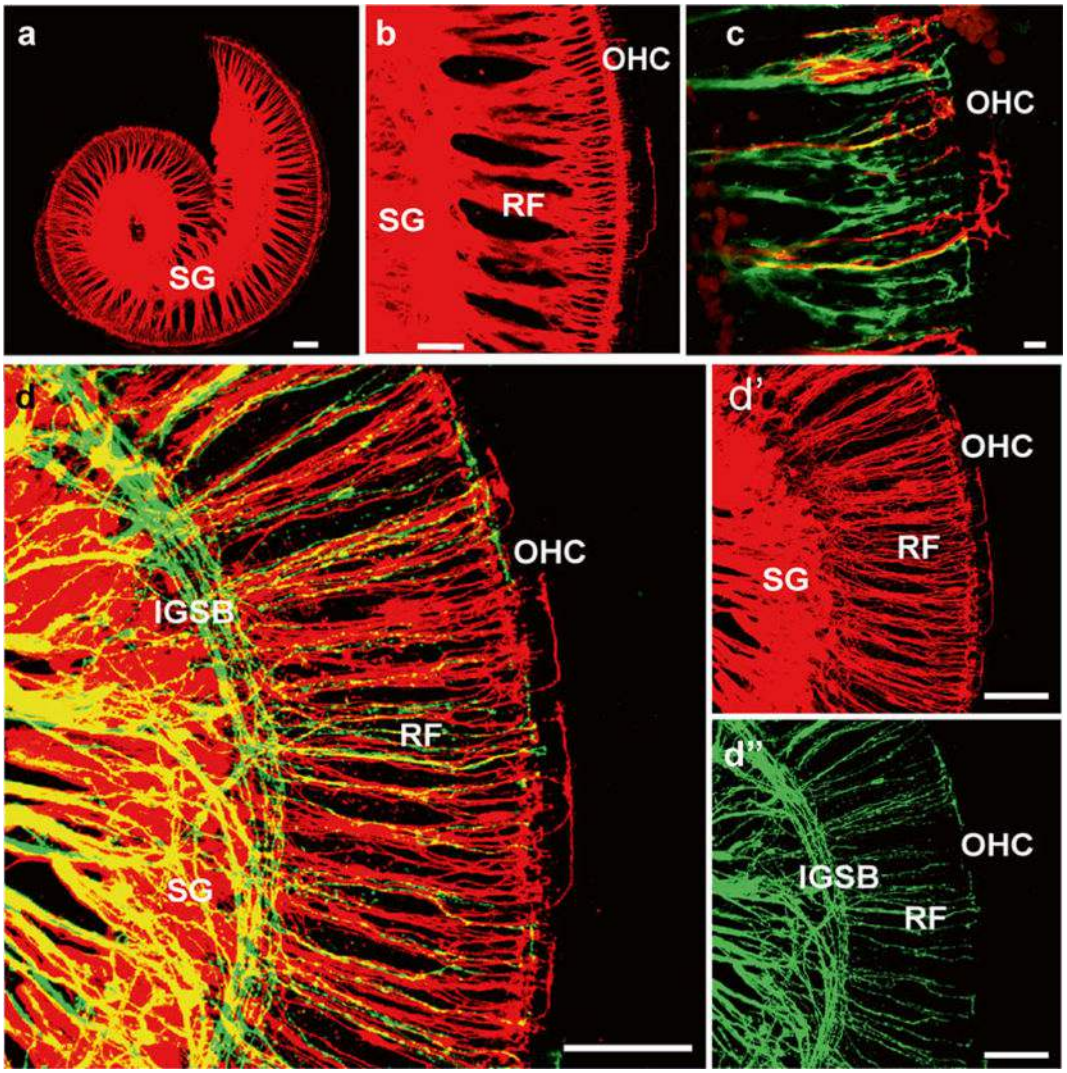

Fig. 2.

Dye labeling of afferent and efferent fiber to the organ of Corti after central applications to cochlear nuclei (NeuroVue Orange, *red*) and crossing efferent fibers (NeuroVue Maroon, *green*). Whole mounted in glycerol and viewed within 1 h after mounting. (**a**, **b**) Single and (**c**, **d**) double labeling of afferents (*red*) and efferents (*green*) to the organ of Corti of a newborn mouse. Labeled spiral ganglion neurons (SG) send radial fibers (RF) to reach the IHC region with few fibers expanding to OHC. Efferents form intraganglionic spiral bundle (IGSB), join radial fibers and reach to IHC but only rarely to OHC. Bar = 100 μm in (**a**, **b**, **d**) 10 μm in (**c**). Modified after [23, 29]

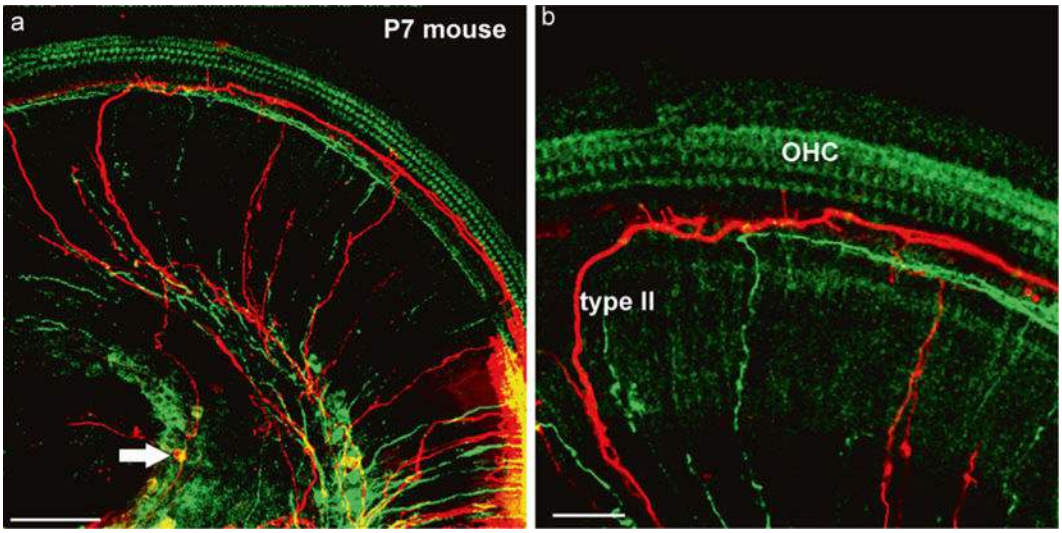

Fig. 3.

Dye labeling of afferents and efferents using peripheral applications. Two different lipophilic dyes (*green, red*) (**a**) were inserted next to each other in the dissected apex of a 7-day-old mouse. Note that both *green* and *red* (*arrow*) spiral ganglion cells are labeled next to the injection site (*lower right* in **a**). Two type II afferents are filled toward the apex before the turn into radial fibers and reach the spiral ganglion neurons (*arrow* in **a**). (**b**) The higher power image shows the fine branches emanating from type II fibers to reach the area of inner hair cells. Bar equals 100 μm in (**a**), 50 μm in (**b**). Modified after [65]

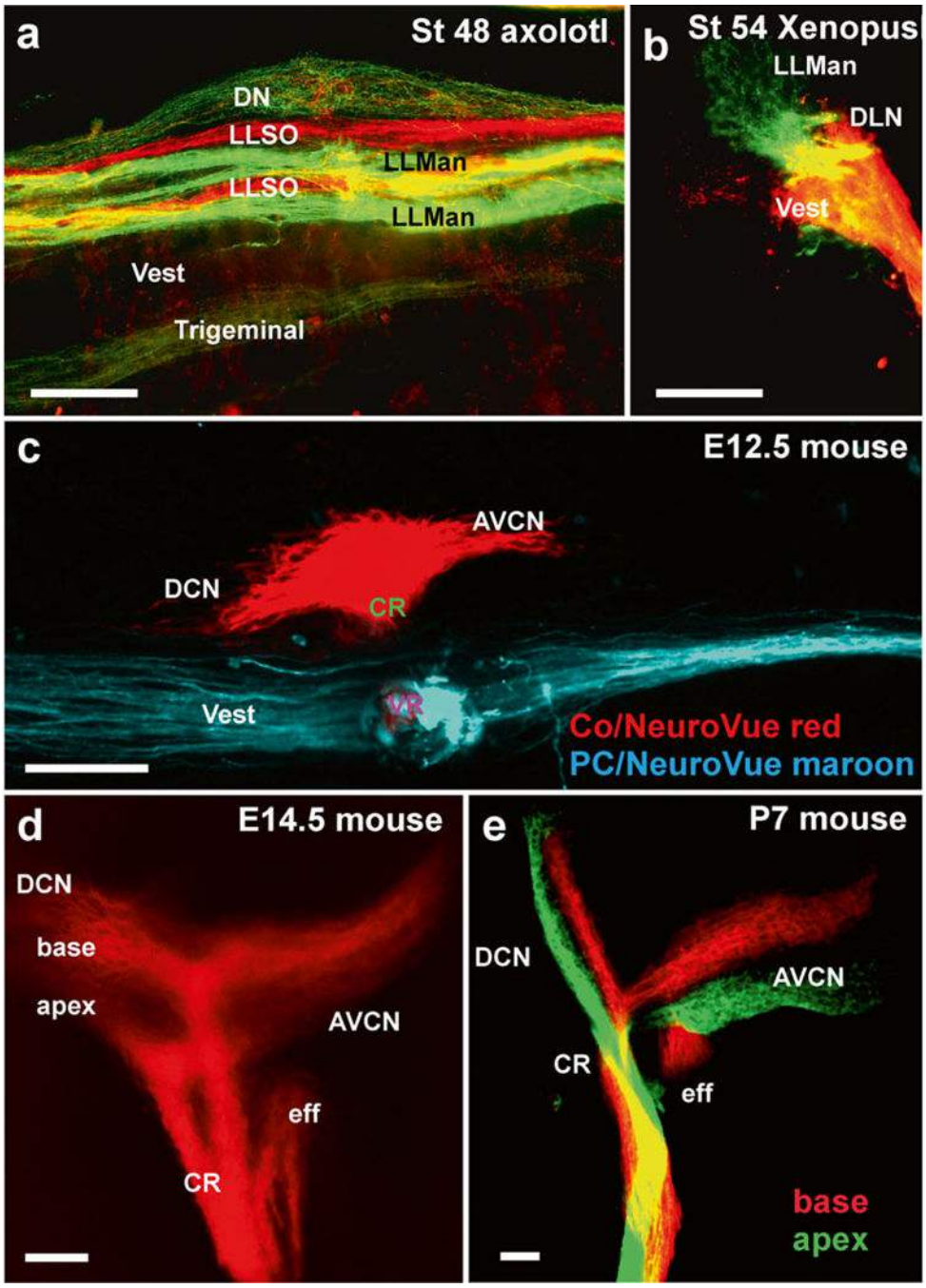

Fig. 4.

Afferent projections revealed by dextran amine and lipophilic dye tracing. (**a**, **b**) Dextran amine can be used effectively to trace different sensory organ innervation to their CNS target. The axolotl brainstem shows the termination of mandibular (LLMan) and supraorbital (LLSO) afferents in two distinct fascicles that may represent the different hair cell polarity. In contrast, afferents from the electroreceptive ampullary organs terminate overlappingly in the dorsal nucleus (DN). Frogs do not have electroreception and their lateral line projections are segregated from vestibular (Ves) and auditory projections to the dorsolateral auditory

nucleus (DLN). (**c**) Inner ear fibers are segregated for the vestibular and cochlear afferents as early as E12.5. (**d**, **e**) Already at E14.5 the basal and apical area of the cochlea project into distinct fascicles, which can also be labeled with different colored dyes. *AVCN* anteroventral cochlear nucleus, *CR* cochlear root, *eff* efferent fibers; DCN dorsal cochlear nucleus, *DLN* dorsolateral nucleus. Bar equals 100 μm, modified after [35, 66]

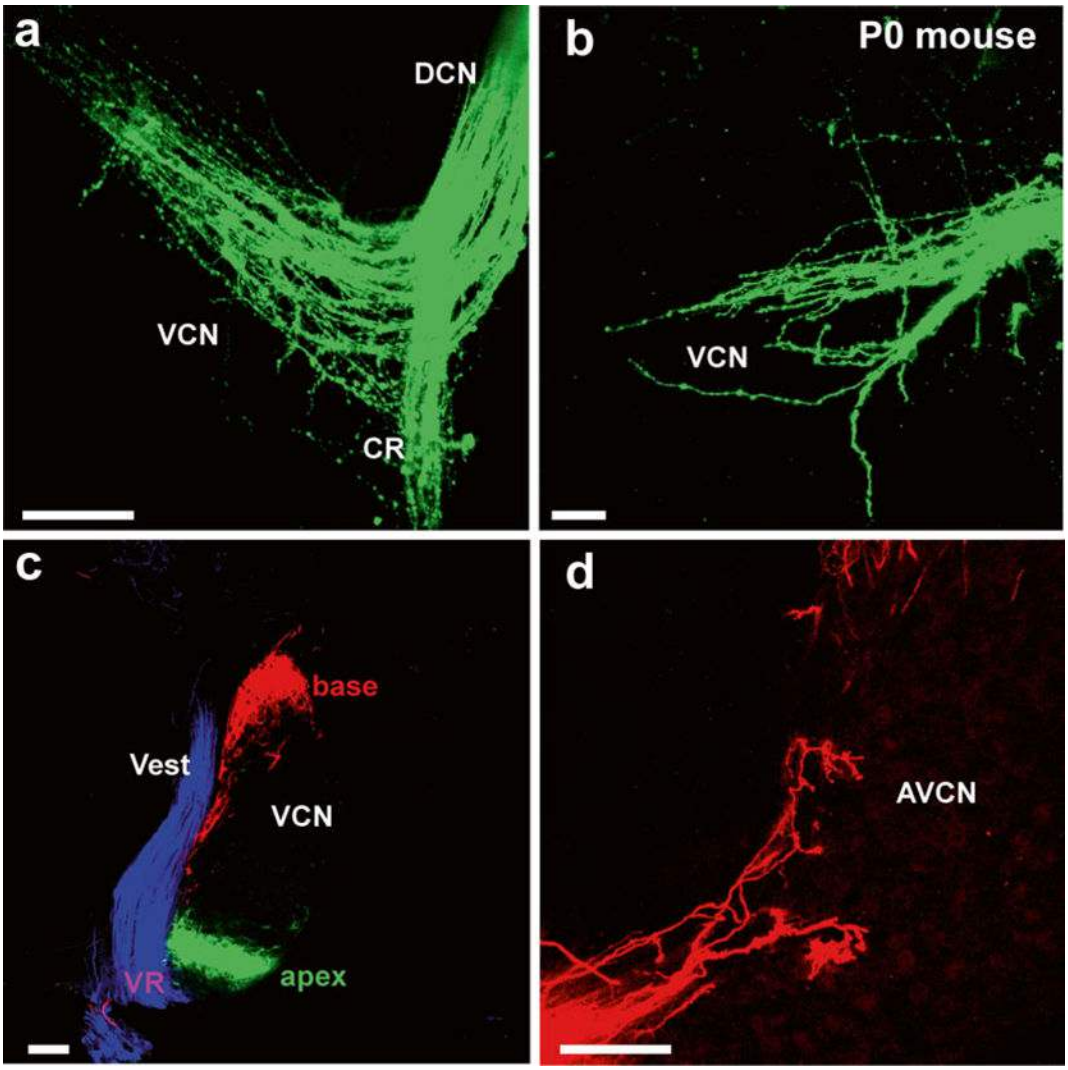

Fig. 5.

Details of afferents to cochlear nuclei revealed in (**a**, **b**) whole mounts and (**c**, **d**) sections. Lipophilic dyes can reveal the pattern of innervation of cochlear afferents and deviations from normal projections in mutant mice (**a**, **b**) or can be used in vibratome sections (**c**) to show the segregation of basal, apical, and vestibular projections to the cochlear nucleus and the nearby vestibular nucleus. (**d**) Higher magnifications show the Golgi-like filling of afferents beginning to form endbulbs of Held. *AVCN* anteroventral cochlear nucleus, *CR* cochlear root, *VCN* ventral cochlear nucleus, *Vest* vestibular nucleus, *VR* vestibular root. Bar equals 100 μm. Modified after [67]

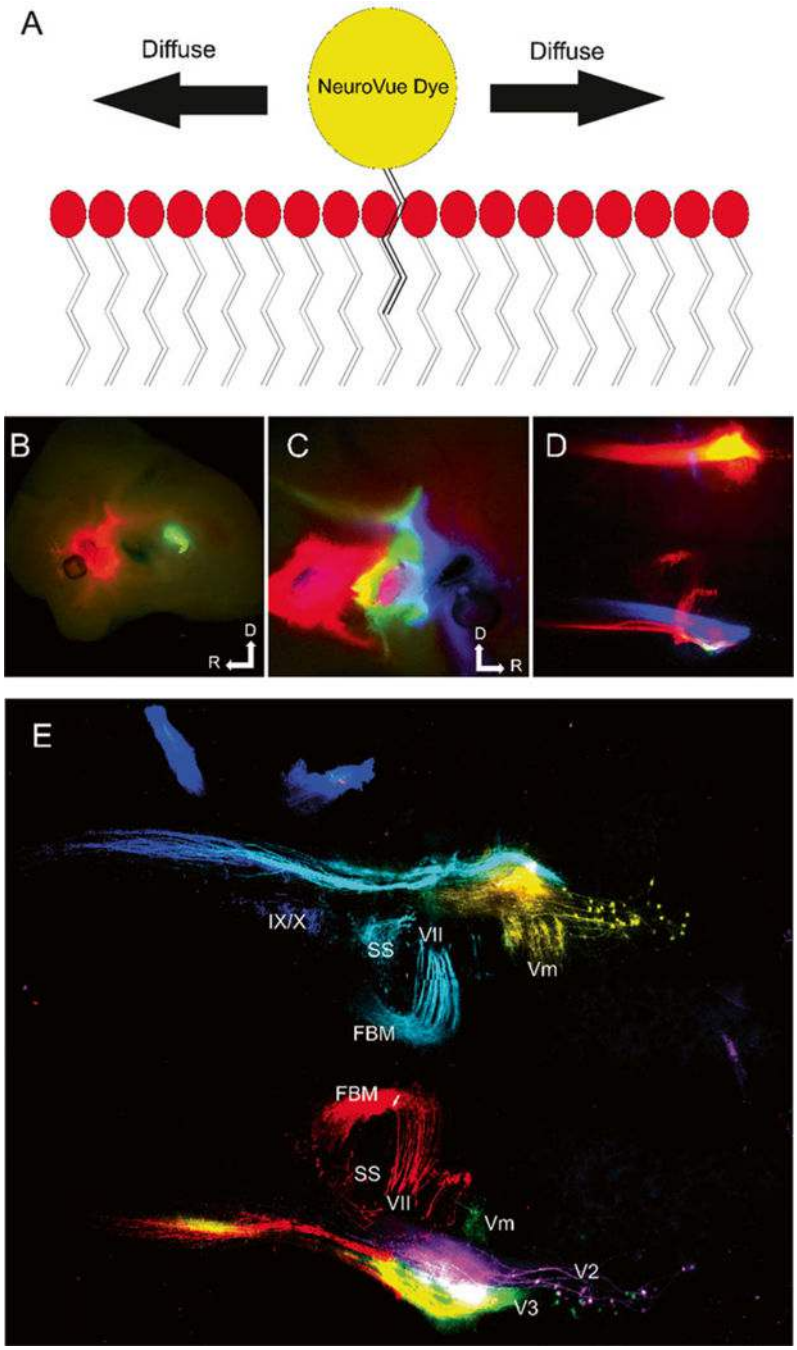

Fig. 6.

Dye diffusion and six-color labeling of NV-labeled cranial nerve distribution in hindbrain. (**a**) Drawing of how NeuroVue labels neurons. When the dye is added to the neuronal membrane, lipophilic chains on the fluorophore become lodged within the lipid bilayer. Through Brownian motion and diffusion gradients the dye is able to diffuse through the bilayer along the entire neuron. The entire cell can be visualized, because the dyes do not rely on actin or subcellular structures. (**b**) E12.5 mouse showing dye injection sites of NVO (*red*), NVB (non-fluorescent), and PTIR334 (*green*) labeling trigeminal (V), facial (VII) and

glossopharyngeal/vagal (IX/X), respectively. Dorsal is up and rostral is to the left. (**c**) Opposite side of same mouse in (**b**) showing dye injections NVM (*blue*), NVJ (*green*), NVR (*red*) labeling the maxillary branch of trigeminal (V2), mandibular branch of trigeminal (V3) and facial nerves (VII), respectively. Dorsal is up and rostral is to the right. (**d**) Hindbrain of same mouse in (**b**) and (**c**) imaged, using conventional epifluorescence to visualize the central projections of labeled nerves. With conventional Texas *red* (566 nm), fluorescein (488 nm), and Cy5 (625 nm) filter cubes, NVO and NVR cannot be distinguished, PTIR334 and NVJ cannot be distinguished, and NVB cannot be imaged. (**e**) Confocal of same hindbrain shown in (**d**); NVO, (*yellow*), NVB (*cyan*), PTIR334 (*blue*), NVM (*magenta*), NVJ (*green*) and NVR (*red*). Modified after [41]